AMERICAN SOCIETY FOR MICROBIOLOGY | Journal of Virology®

VIRUS-CELL INTERACTIONS

A Cysteine Residue of Human Cytomegalovirus vMIA Protein Plays a Crucial Role in Viperin Trafficking to Control Viral Infectivity

Jeong Jin Kim,[a] Sookyung Hong,[a] Jun-Young Seo[a]

[a]Severance Biomedical Science Institute, Graduate School of Medical Science, Brain Korea 21 Project, Yonsei University College of Medicine, Seoul, Republic of Korea

ABSTRACT Viperin is a multifunctional interferon-inducible protein that is directly induced in cells by human cytomegalovirus (HCMV) infection. The viral mitochondrion-localized inhibitor of apoptosis (vMIA) interacts with viperin at the early stages of infection and translocates it from the endoplasmic reticulum to the mitochondria, where viperin modulates the cellular metabolism to increase viral infectivity. Viperin finally relocalizes to the viral assembly compartment (AC) at late stages of infection. Despite the importance of vMIA interactions with viperin during viral infection, their interacting residues are unknown. In the present study, we showed that cysteine residue 44 (Cys44) of vMIA and the N-terminal domain (amino acids [aa] 1 to 42) of viperin are necessary for their interaction and for the mitochondrial localization of viperin. In addition, the N-terminal domain of mouse viperin, which is structurally similar to that of human viperin, interacted with vMIA. This indicates that the structure, rather than the sequence composition, of the N-terminal domain of viperin, is required for the interaction with vMIA. Recombinant HCMV, in which Cys44 of vMIA was replaced by an alanine residue, failed to translocate viperin to the mitochondria at the early stages of infection and inefficiently relocalized it to the AC at late stages of infection, resulting in the impairment of viperin-mediated lipid synthesis and a reduction in viral replication. These data indicate that Cys44 of vMIA is therefore essential for the intracellular trafficking and function of viperin to increase viral replication. Our findings also suggest that the interacting residues of these two proteins are potential therapeutic targets for HCMV-associated diseases.

IMPORTANCE Viperin traffics to the endoplasmic reticulum (ER), mitochondria, and viral assembly compartment (AC) during human cytomegalovirus (HCMV) infection. Viperin has antiviral activity at the ER and regulates cellular metabolism at the mitochondria. Here, we show that Cys44 of HCMV vMIA protein and the N-terminal domain (aa 1 to 42) of viperin are necessary for their interaction. Cys44 of vMIA also has a critical role for viperin trafficking from the ER to the AC via the mitochondria during viral infection. Recombinant HCMV expressing a mutant vMIA Cys44 has impaired lipid synthesis and viral infectivity, which are attributed to mislocalization of viperin. Cys44 of vMIA is essential for the trafficking and function of viperin and may be a therapeutic target for HCMV-associated diseases.

KEYWORDS viperin, vMIA, HCMV, interferon-inducible protein, interacting residues, intracellular trafficking

Human cytomegalovirus (HCMV) is a member of the betaherpesvirus family and is an opportunistic pathogen that is highly prevalent worldwide (1). It rarely exhibits pathogenic symptoms in healthy individuals but causes severe disease in immunocompromised individuals. HCMV is a major cause of morbidity and mortality, causes allograft rejection in transplant recipients, and leads to congenital diseases, including neurological defects in infants (2, 3). HCMV triggers a wide range of viral and cellular

Editor Felicia Goodrum, The University of Arizona

Address correspondence to Jun-Young Seo, jyseo0724@yuhs.ac.

The authors declare no conflict of interest.

Received 5 December 2022
Accepted 22 May 2023
Published 12 June 2023

events, including viral assembly and replication, transcriptional activation, and host cellular modulation during viral infection (4, 5). HCMV also regulates the host cellular metabolism to enhance viral infectivity (6–8). HCMV-induced glycolytic and lipogenic activations are mediated by viperin, which is a host protein that is directly induced by HCMV infection (9, 10).

Viperin (also known as RSAD2 or cytomegalovirus-induced gene 5 protein) is an interferon (IFN)-inducible protein (11) that has multiple roles in various cell types, including macrophages, fibroblasts, dendritic cells, adipocytes, and astrocytes (9, 12–17). Viperin exhibits antiviral activity against many viruses (12–15), mediates signaling pathways to produce IFNs, IFN-stimulated genes (ISGs), and cytokines (17–19), and controls cellular metabolism (9, 10, 16). During HCMV infection, viperin exerts distinct functions depending on its intracellular localization (9, 20). Viperin traffics to three cellular compartments during infection: the endoplasmic reticulum (ER), the mitochondria, and the viral assembly compartment (AC) (9, 20). When viperin is preexpressed prior to HCMV infection, it localizes to the ER, where it inhibits viral replication by blocking the ER-to-Golgi trafficking of soluble but not membrane-associated viral proteins, such as gB, pp65, and pp28 (20, 21). When viperin expression is induced directly by HCMV at the early stages of infection, the viral protein vMIA (viral mitochondrion-localized inhibitor of apoptosis) binds to viperin and translocates it from the ER to the mitochondria, where it interacts with mitochondrial trifunctional protein (TFP) and modulates cellular energy and lipid metabolism to facilitate viral infectivity (9, 10). Viperin finally relocalizes to the AC at the late stages of infection (20), although its function in the AC remains unknown. Given that viperin function is closely associated with its intracellular localization, the interaction between HCMV vMIA protein and viperin plays an essential role in determining viperin function during viral infection.

vMIA is encoded by the UL37 exon 1 (UL37x1) gene of HCMV (22, 23). It is synthesized in the ER, and predominantly localized to the mitochondria (24–26). vMIA inhibits stimulus-induced apoptosis (22, 27–31) and mediates the cytopathic effects of HCMV infection by modulating mitochondrial bioenergetics (32). vMIA also localizes to the peroxisomes, where it induces peroxisomal fragmentation and morphological changes and suppresses the IFN-independent production of ISGs (33). vMIA also plays a role as a vehicle to transport viperin to the mitochondria during HCMV infection. vMIA interactions with viperin are important for driving the proviral function of viperin (9, 10). However, the precise residues of vMIA that interact with viperin are unknown, and the mechanism of action is currently unclear.

In the present study, we identified the interacting residues between vMIA and viperin in order to reveal their role in the trafficking and the function of viperin during HCMV infection by generating a series of mutants. We also verified these potential interacting residues by performing additional functional assays. By identifying the interacting residues between viperin and vMIA, we have expanded our understanding of virus-host interaction, which is crucial for the intracellular trafficking and function of viperin and may help provide potential targets for anti-HCMV therapies.

RESULTS

Cys44 of vMIA and the N-terminal domain of viperin are required for their interaction. Viperin traffics from the ER to the mitochondria by interacting with vMIA in the early stages of HCMV infection (9). To determine which domain of vMIA is responsible for the interaction with viperin, we initially generated a series of vMIA mutants (Fig. 1A; see Fig. S1A in the supplemental material). Transient transfection and coimmunoprecipitation experiments revealed that viperin strongly interacts with amino acids (aa) 1 to 44 of vMIA, but not aa 1 to 39 of vMIA (Fig. 1B). This indicates that aa 40 to 44 of vMIA are important for the interaction with viperin. This segment consists of three lysine residues (aa 40 to 42), an alanine residue (aa 43), and a cysteine residue (aa 44). Lysine is a positively charged basic amino acid that plays important roles in protein stability by forming electrostatic interactions. Cysteine residues also play essential roles in protein structure and function by conferring stability through disulfide bond formation and maintaining proper maturation and localization through protein-protein intermolecular interactions (34–37). Therefore, we

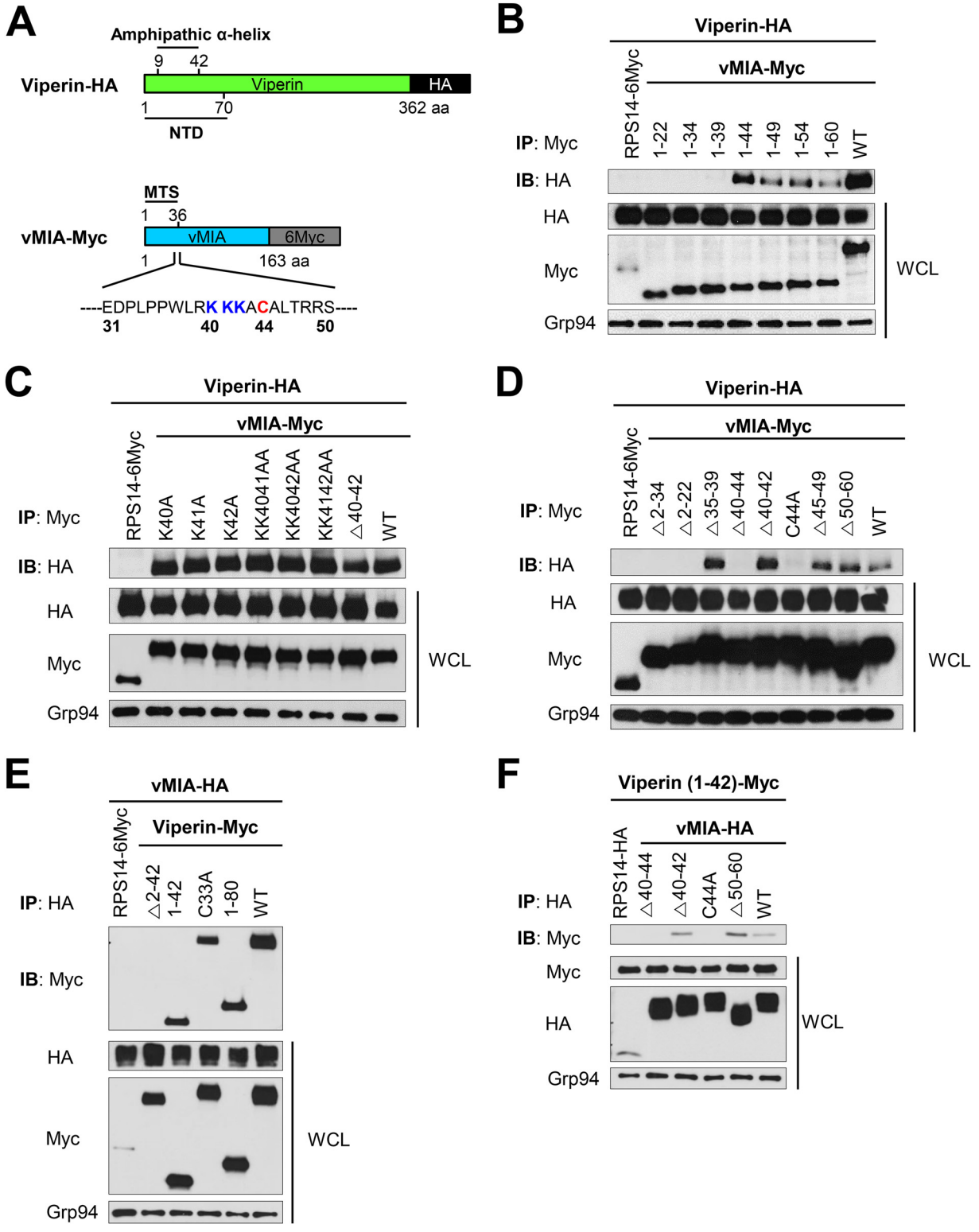

FIG 1 Cys44 of vMIA and the N-terminal domain of viperin are essential for their interaction. (A) Constructs of HA-tagged viperin and Myc-tagged vMIA. The N-terminal domain (NTD, residues 1 to 70) and an amphipathic α-helix (residues 9 to 42) of viperin and the N-terminal mitochondrial targeting sequence (MTS, residues 2 to 36) of vMIA are shown. The amino acid sequence of vMIA is listed from aa 31 to 50, with Lys40-42 and Cys44 shown in blue and red, respectively. (B to F) HEK-293T cells were transiently cotransfected with the indicated constructs for 24 h: (B) viperin wild type (WT) and vMIA truncation mutants, (C) viperin WT and vMIA substitution mutants, (D) viperin WT and vMIA deletion mutants, (E) vMIA WT and viperin mutants, and (F) the N-terminal domain of viperin and vMIA mutants. Coimmunoprecipitation was performed, and each protein was detected by immunoblotting using specific monoclonal antibodies. Ribosomal protein subunit 14 (RPS14) was used as a negative control, and Grp94 was used as the loading control. WCL, whole-cell lysate.

suspected that the three lysine residues (aa 40 to 42) or the cysteine residue (aa 44) of vMIA might be important for binding to viperin. Viperin interacted with vMIA mutants in which one or two lysine residues within aa 40 to 42 of vMIA were replaced by alanine residues (Fig. 1C), indicating that the lysine residues of vMIA are not necessary for the interaction with viperin. However, viperin did not interact with vMIA mutants in which the cysteine residue (aa 44) was deleted or replaced by an alanine residue, or with vMIA mutants lacking a mitochondrial targeting sequence (MTS) (MTS full length, aa 2 to 36; MTS α subunit, aa 2 to 22) (26) (Fig. 1D). This suggests that the cysteine residue 44 (Cys44) and the MTS of vMIA are required for binding to viperin. Then, to identify which domain of viperin is necessary for the interaction with vMIA, we constructed a series of viperin mutants (Fig. S1B). All mutants, except for one lacking the N-terminal domain (Δ2 to 42) of viperin, interacted with vMIA (Fig. 1E), indicating that the N-terminal domain is required for this interaction. The N-terminal domain of viperin has a cysteine residue (aa 33). We expected that the Cys33 of viperin might form a disulfide bond with Cys44 of vMIA. However, the Cys33 of viperin was not required for binding to vMIA (Fig. 1E). To further confirm the interacting domains of viperin and vMIA, we tested whether viperin expressing only the N-terminal domain (aa 1 to 42) binds to vMIA mutants (Fig. S1C). As anticipated, this viperin mutant (aa 1 to 42) bound to only vMIA mutants containing Cys44 (Fig. 1F). Taken together, these data indicate that Cys44 of vMIA and the N-terminal domain (aa 1 to 42) of viperin are essential for their interaction.

Cys44 of vMIA is critical for translocating viperin into the mitochondria. To determine whether Cys44 of vMIA affects the intracellular localization of viperin, we performed confocal microscopy on cells transiently expressing vMIA and/or viperin mutants. All vMIA mutants, except for the mutant lacking the MTS domain (Δ2 to 34), were normally localized to the mitochondria in transiently transfected HeLa cells (Fig. S2A). The N-terminal domain of viperin is crucial for its localization to the cytosolic face of the ER (21). Consistent with previous reports, in the present study all viperin mutants, except for the mutant lacking its N-terminal domain (Δ2 to 42), were predominantly localized to the ER in transiently transfected cells (Fig. S2B). Meanwhile, viperin traffics from the ER to the mitochondria by interacting with vMIA (9). We observed that viperin was colocalized with vMIA to the mitochondria in mutants that included the Cys44 residue in transiently cotransfected cells. However, viperin was not translocated from the ER to the mitochondria when it was coexpressed with vMIA mutants lacking the MTS domain or Cys44 of vMIA (Fig. 2A, Fig. S2C). Mitochondrial localization of viperin and vMIA mutants was further evaluated by cellular fractionation (38, 39). HEK-293T cells transiently cotransfected with viperin and vMIA wild type (WT) or vMIA Cys44 mutant were lysed and subjected to subcellular fractionation. Each protein in the mitochondrial and cytosolic fractions was detected by immunoblotting (Fig. 2B). Consistent with the results of confocal microscopy, viperin was found in the mitochondrial fraction when coexpressed with vMIA WT but not the vMIA Cys44 mutant. Similarly, vMIA was colocalized in the mitochondria with viperin mutants expressing the N-terminal domain (Fig. 2C). We also confirmed that the viperin mutant expressing only the N-terminal domain could still colocalize with vMIA, except for the vMIA Cys44 mutant (Fig. 2D). Additionally, similar intracellular localization patterns of vMIA and/or viperin mutants were observed in Cos-7 cells (data not shown). Taken together, these data indicate that Cys44 of vMIA and the N-terminal domain of viperin are essential for trafficking of viperin from the ER to the mitochondria.

The structure of the N-terminal domain of viperin is necessary for its interaction with vMIA. Viperin is highly conserved, even between distantly related vertebrates, and viperin-like enzymes are also expressed in fungi, bacteria, and archaea (11, 40, 41). The N-terminal domain of viperin contains an amphipathic α-helix, but its length and sequence vary between species (11). The N-terminal domain of human viperin is structurally similar to that of mouse viperin, but its sequence is different (Fig. 3A). To determine whether viperin interactions with vMIA depend on the structure or sequence composition of the N-terminal domain, we generated a series of mouse viperin mutants. As with human viperin mutants, all the mouse viperin mutants except for the mutant lacking the N-terminal domain (Δ2 to 42) interacted with vMIA, and colocalized to the mitochondria in transiently

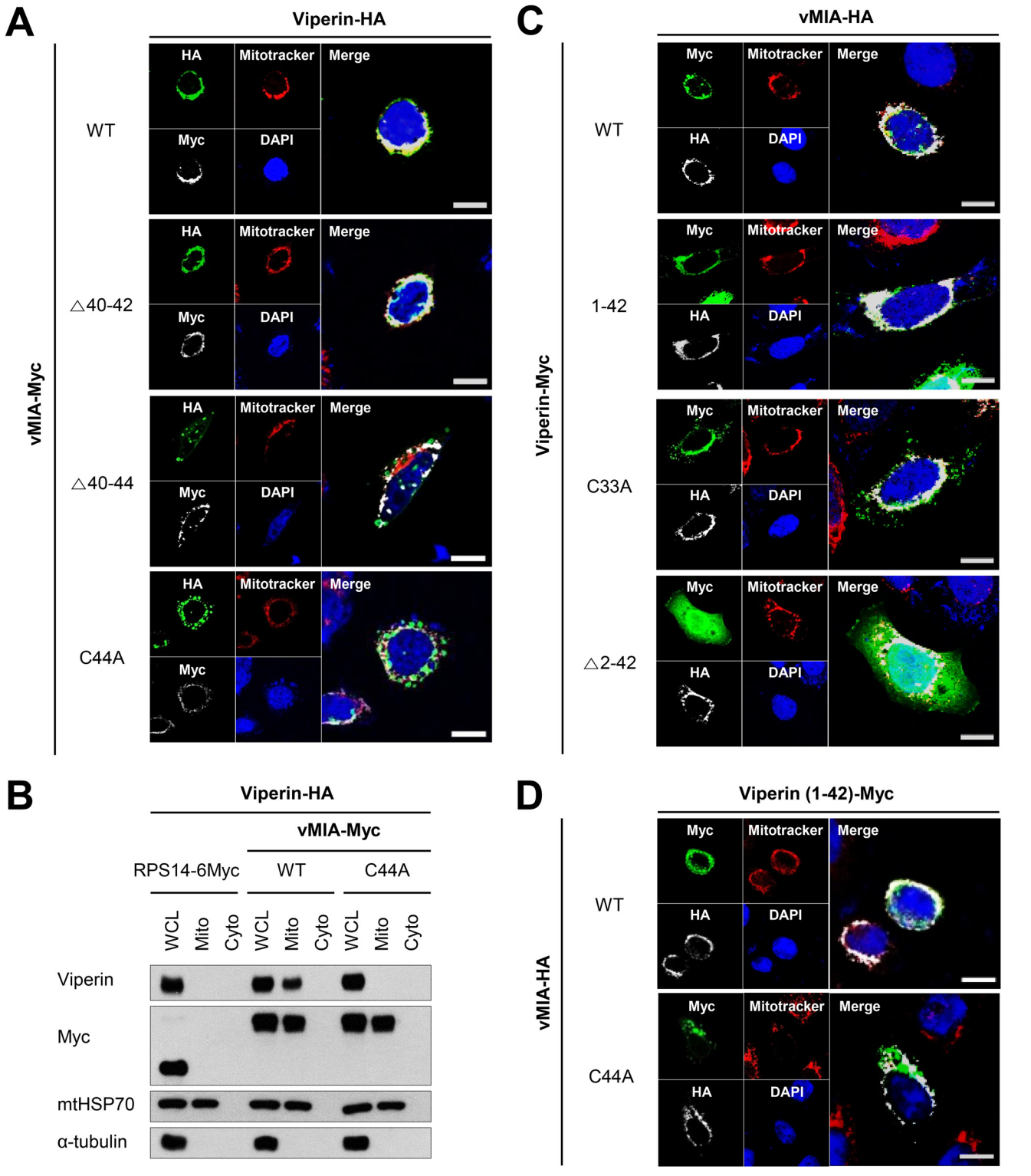

FIG 2 Cys44 of vMIA is required for the mitochondrial localization of viperin. (A) HeLa cells were transiently cotransfected with viperin WT and vMIA mutants. Cells were stained with anti-HA and anti-myc antibodies, with MitoTracker Red as the mitochondrial indicator. DAPI (4′,6-diamidino-2-phenylindole) was used to stain the nuclei. A representative image from two independent experiments is shown. Scale bar = 10 μm. (B) HEK-293T cells were transiently cotransfected with viperin and vMIA WT or mutant (C44A) for 24 h. Cells were lysed and subjected to subcellular fractionation. Each protein in mitochondrial (Mito) and cytosolic (Cyto) fractions was detected by immunoblot using specific monoclonal antibodies. Ribosomal protein subunit 14 (RPS14) was used as a negative control. mtHSP70 and α-tubulin were used as mitochondrial and cytoplasmic markers, respectively. WCL, whole-cell lysate. (C and D) HeLa cells were transiently cotransfected with the indicated constructs: (C) vMIA WT and viperin mutants and (D) the N-terminal domain of viperin and vMIA WT or mutant (C44A). Cells were stained with anti-HA and anti-myc antibodies, with MitoTracker Red as the mitochondrial indicator. DAPI was used to stain the nuclei. A representative image from two independent experiments is shown. Scale bar = 10 μm.

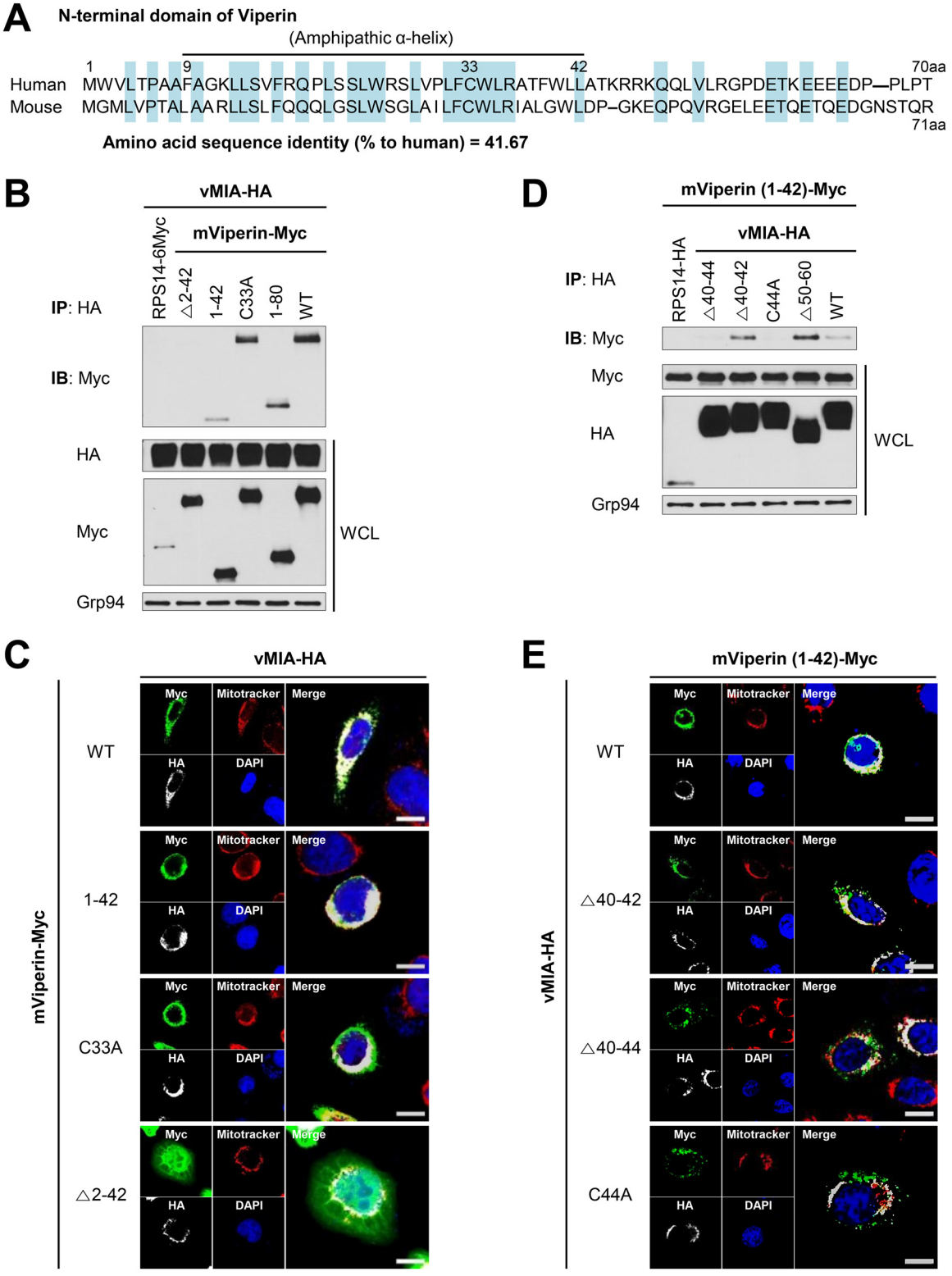

FIG 3 The N-terminal domain of mouse viperin interacts with Cys44 of vMIA. (A) The amino acid alignment of human and mouse viperin. Shared amino acid residues are shaded in blue. The amphipathic α-helix, which is shared among mammals, extends from residues 9 to 42. (B) HEK-293T cells were transiently cotransfected with vMIA WT and mouse viperin mutants for 24 h. (B) coimmunoprecipitation was performed, and each protein was detected by immunoblotting using specific monoclonal antibodies. Ribosome protein subunit 14 (RPS14) was used as a negative control, and Grp94 was used as the loading control. WCL, whole-cell lysate. (C) Cells were stained with anti-HA and anti-myc antibodies, with MitoTracker Red as the mitochondrial indicator. DAPI was used to stain the nuclei. A representative image from two independent experiments is shown. Scale bar = 10 μm. HEK-293T cells

(Continued on next page)

transfected HeLa cells (Fig. 3B and C). We also confirmed that a mouse viperin mutant expressing only the N-terminal domain interacted with vMIA mutants containing Cys44 and trafficked to the mitochondria (Fig. 3D and E). These data indicate that the structure, rather than the sequence composition, of the N-terminal domain of viperin is required for its interaction with vMIA.

Cys44 of vMIA is crucial for viperin trafficking during HCMV replication. Thereafter, to investigate the effect of vMIA Cys44 on its interaction with viperin during HCMV infection, we created a panel of recombinant HCMVs in which several residues of vMIA were deleted or substituted and a series of revertant HCMVs, in which the vMIA mutants were rescued by the vMIA WT, using mutagenesis in the bacterial artificial chromosome (BAC) pHB15-containing HCMV strain AD169 (kindly provided by T. Stamminger, Ulm University Medical Center) (42) (Fig. S3A and B). Due to limitations in antibody availability, we also generated hemagglutinin (HA)-tagged recombinant HCMVs, in which the HA-tag sequence was inserted between the alternative splicing site and the stop codon of vMIA (UL37x1), which encode the HA-tag for vMIA but not the full length of pUL37 (Fig. S3B). To ensure correct targeting of recombination to the desired HCMV genomic location, the recombinant BAC DNA was digested with BamHI and electrophoresed. Fragments distinguishing the inserted KAN^r cassette from the vMIA mutant in the target region were observed (Fig. S3C). Nucleotide sequence analysis of the PCR products amplified from these recombinant BACs confirmed the correct insertion of the mutant. All recombinant HCMVs were harvested and amplified. The expression levels of viral proteins IE1 and vMIA mutants or vMIA-HA mutants and viperin in cells infected with these recombinant viruses were similar (Fig. S4A and B). There was no difference in the expression levels of viral proteins IE1 and vMIA and viperin between cells infected with HCMV WT and cells infected with HA-tagged HCMV (HCMV-vMIA-HA) (Fig. S4C), indicating that HA-tagged recombinant HCMVs are suitable for downstream assays. Consistent with the results of transiently transfected cells (Fig. 1D), an immunoprecipitation assay showed that Cys44 of vMIA is required for binding to endogenous viperin in virus-infected cells (Fig. 4A). Having previously observed that viperin traffics to three distinct cellular compartments during HCMV infection (20), we next determined if vMIA Cys44 is responsible for viperin trafficking during viral replication. Confocal microscopy did not detect viperin in the mitochondria at 1 day postinfection (dpi) in cells infected with the recombinant HCMV encoding a vMIA mutant in which Cys44 is replaced by alanine, although vMIA normally localizes to the mitochondria (Fig. 4B, Fig. S4D). Conversely, viperin was observed in the mitochondria at 1 dpi in cells infected with revertant viruses. We further evaluated the mitochondrial localization of viperin in cells infected with the recombinant HCMVs by cellular fractionation. Virus-infected cells were lysed and subcellular fractionation was performed at 1 dpi. Each protein in the mitochondrial and cytosolic fractions was detected by immunoblotting (Fig. 4C). Consistent with the results of confocal microscopy, viperin was found in the mitochondrial fraction of cells infected with the HCMV WT and the revertant virus but not the recombinant HCMV encoding the vMIA Cys44 mutant. vMIA Cys44 is therefore a critical amino acid for the mitochondrial targeting of viperin in the early stages of infection. Interestingly, the recombinant HCMV encoding the vMIA Cys44 mutant had impaired viperin localization to the AC at late stages of infection (5 dpi) (Fig. 4D). The efficiency of viperin trafficking to the AC was reduced by about half in cells infected with the recombinant HCMV encoding the vMIA Cys44 mutant compared with in cells infected with the HCMV WT, and this was restored in cells infected with the revertant virus (Fig. 4D). These results indicate that the mitochondrial localization of viperin immediately after infection is a prerequisite for its relocalization to the AC at later stages of infection, suggesting that viperin travels to the AC mainly via the mitochondria instead of the ER during HCMV infection.

FIG 3 Legend (Continued)
were transiently cotransfected with the N-terminal domain of mouse viperin and vMIA mutants for 24 h. (D) coimmunoprecipitation and immunoblotting were performed with the indicated antibodies. (E) Cells were stained with anti-HA and anti-myc antibodies, with MitoTracker Red as the mitochondrial indicator. A representative image from two independent experiments is shown. Scale bar = 10 μm.

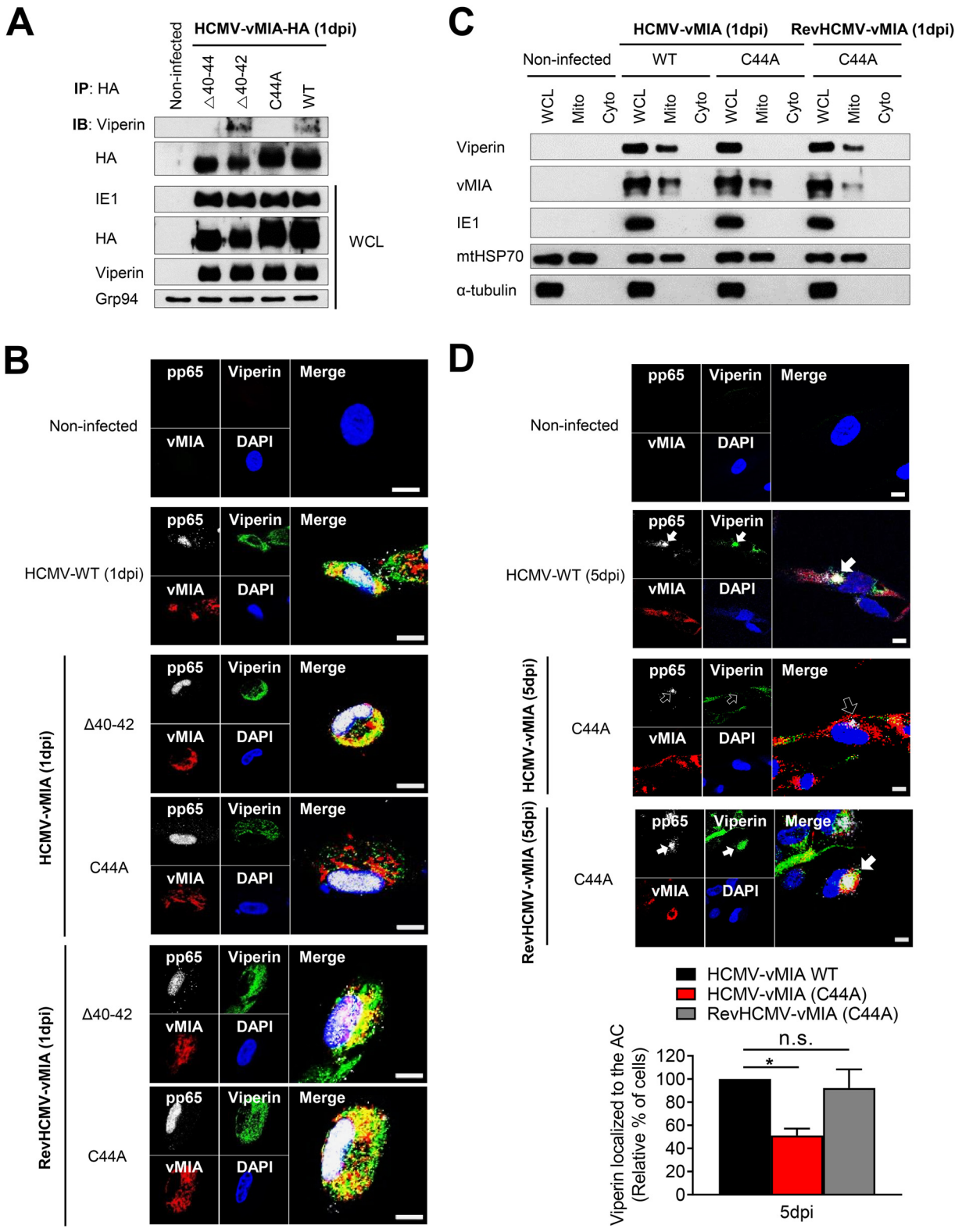

FIG 4 Recombinant HCMV expressing the Cys44 vMIA mutant has impaired viperin trafficking during viral infection. (A) The interaction between the vMIA mutant of the recombinant virus and endogenous viperin. HFF cells were infected with the recombinant HCMV expressing the HA-tagged vMIA mutant at an MOI of 1. At 1 day postinfection (dpi), coimmunoprecipitation was performed, and each protein was detected by immunoblotting using specific monoclonal antibodies. HCMV protein IE1 was used as the control for viral protein expression, and Grp94 was used as the loading control. WCL, whole cell-lysate. (B and C) Intracellular localization of the vMIA mutant of the recombinant virus and endogenous viperin at the early stages of infection. HFF cells were infected with the recombinant HCMV at an MOI of 1 for 1 day. (B) Cells were stained with antibodies specific to viperin and

(Continued on next page)

vMIA Cys44 is essential for viperin function to increase viral infectivity. Viperin translocation to the mitochondria enables it to interact with and block the function of mitochondrial trifunctional protein (TFP), which mediates fatty acid-β-oxidation, resulting in decreased cellular ATP levels and disruption of the actin cytoskeleton and thus facilitating viral infectivity (9). We therefore determined if the elimination of Cys44 of vMIA, which is responsible for viperin trafficking, would affect HCMV replication. We measured the kinetics of replication for recombinant viruses from human foreskin fibroblasts (HFFs) by performing a multistep growth assay. Viral infectivity was significantly reduced by more than 10-fold in cells infected with the recombinant HCMV encoding the Cys44 vMIA mutant compared with the HCMV WT, and this was restored in cells infected with the revertant virus (Fig. 5A). This indicates that viperin's interaction with vMIA enables it to enhance viral replication. To test whether mutation of Cys44 in vMIA affects the function of intact vMIA in viral replication, we analyzed mitochondrial morphogenesis and apoptosis in cells infected with the recombinant viruses. Small punctate mitochondrial staining was observed in cells infected with the HCMV WT, the recombinant HCMV encoding the Cys44 vMIA mutant, or the revertant virus, whereas tubular and elongated mitochondrial staining was detected in noninfected cells, indicating that the Cys44 vMIA mutant, like vMIA WT, can induce mitochondrial fragmentation (Fig. S5A). In addition, cell viability and apoptosis inhibition of cells infected with the recombinant HCMV encoding the Cys44 vMIA mutant did not differ from cells infected with the HCMV WT but increased compared with cells infected with a recombinant HCMV deficient in vMIA (HCMV-ΔvMIA) (Fig. S5B). The results indicate that the Cys44 vMIA mutant specifically abrogates viperin-dependent but not viperin-independent functions. Viperin increases fatty acid biosynthesis during HCMV infection, which leads to the accumulation of lipids that are used for the formation of the viral envelope (10). We next measured the expression levels of key lipogenic enzymes acetyl-coenzyme A carboxylase (ACC) 2, fatty acid synthase (FAS), and diacylglycerol acyltransferase (DGAT) 2. The increase in the expression levels of all measured transcripts was significantly less in cells infected with the recombinant HCMV encoding the Cys44 vMIA mutant than in cells infected with the HCMV WT (Fig. 5B). Increased lipogenic enzyme levels upon HCMV infection resulted in the enhancement of lipid synthesis and the accumulation of lipid droplets (LD), which act as a storage compartment for triglycerides and long-chain fatty acids (43–46). We therefore measured the levels of neutral lipids synthesized in the recombinant virus-infected cells. Neutral lipid levels in cells infected with the HCMV WT increased by 2-fold compared with noninfected cells, whereas no change was observed in cells infected with the recombinant HCMV encoding the Cys44 vMIA mutant (Fig. 5C). We also examined the formation of LDs in cells infected with the recombinant viruses. The number and size of LDs were significantly reduced in cells infected with the recombinant HCMV encoding the Cys44 vMIA mutant compared with cells infected with the HCMV WT (Fig. 5D and E). These metabolic alterations were also restored in cells infected with revertant viruses (Fig. 5B to E). To determine whether these phenomena are reproduced when vMIA mutants are overexpressed at similar levels during viral infection, we generated immortalized human fibroblasts (HFtelos) stably expressing a series of vMIA deletion and substitution mutants with or without HA-tag, as previously described (9). The pro-

FIG 4 Legend (Continued)
HCMV proteins vMIA and pp65. pp65 represents a stage of infection that is localized to the nucleus at early stages of infection and to the assembly compartment (AC) at late stages of infection. DAPI was used to stain the nuclei. A representative image from two independent experiments is shown. Scale bar = 10 μm. (C) Cells were lysed and subjected to subcellular fractionation. Each protein in mitochondrial (Mito) and cytosolic (Cyto) fractions was detected by immunoblotting using specific monoclonal antibodies. Noninfected cells were used as a negative control. HCMV protein IE1 was used as the control for viral protein expression. mtHSP70 and α-tubulin were used as mitochondrial and cytoplasmic markers, respectively. WCL, whole-cell lysate. (D) Intracellular localization of the vMIA mutant of the recombinant virus and endogenous viperin at the late stages of infection. HFF cells were infected with the recombinant HCMV at an MOI of 1 for 5 days. Cells were stained with antibodies specific to viperin and HCMV proteins vMIA and pp65. DAPI was used to stain the nuclei. Closed arrows indicate ACs in which viperin and pp65 are colocalized, and open arrows indicate ACs in which pp65 but not viperin is localized. A representative image from two independent experiments is shown. Scale bar = 10 μm. The efficiency of viperin localization to the AC in cells infected with the recombinant virus was quantified. Multiple frames from each coverslip were observed and imaged. A total of 50 to 100 cells displaying pp65-localized AC were counted in each frame (>20 frames/coverslip) and calculated as the ratio of cells with viperin-localized AC to cells with pp65-localized AC. As a control, the ratio in cells infected with HCMV WT was set to 100%. Data are presented as the mean $\pm$ SEM of duplicate samples and are representative of three independent experiments. Statistical analysis was performed by one-way ANOVA with Dunnett's multiple-comparison test. *, $P < 0.05$.

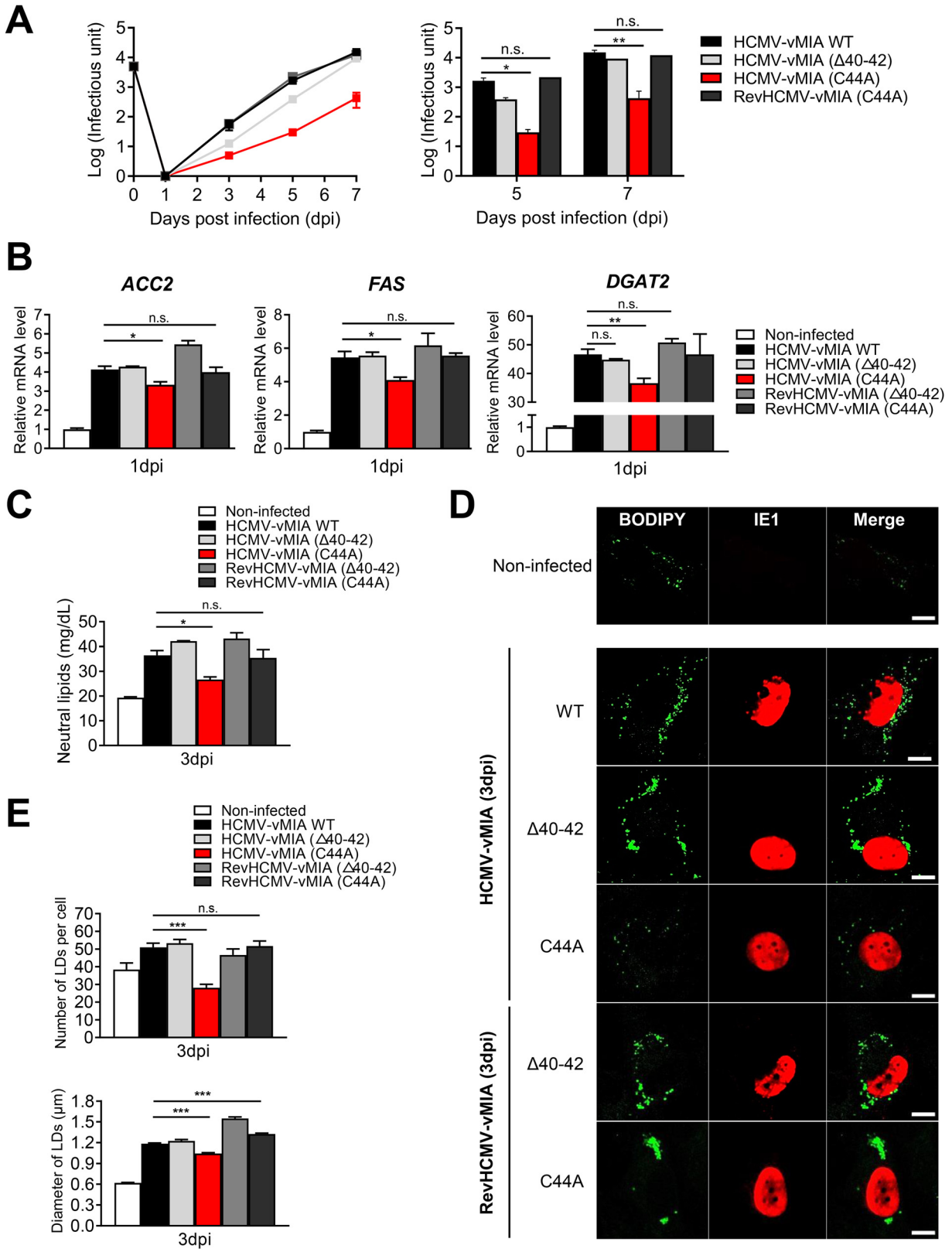

FIG 5 Cys44 of vMIA is required for viperin-dependent lipid synthesis and virion production. (A) HFF cells were infected with the recombinant HCMV at an MOI of 0.05 for the indicated duration. Virus yield was quantified by a fluorescence-based viral infectivity assay. (B) Relative mRNA levels of lipogenic enzymes in HFF cells infected with the recombinant HCMV at an MOI of 1 for 1 day. ACC2, acetyl-coenzyme A (CoA) carboxylase 2; FAS, fatty acid synthase; DGAT2, diacylglycerol acyltransferases 2. HFF cells were infected with the recombinant virus at an MOI of 1 for 3 days: (C) quantification of total neutral lipids. Total neutral lipids from 3×10^6 cells were extracted and quantified using a fluorescence-based lipid assay

(Continued on next page)

tein expression of vMIA mutants was detected in these stable cell lines, whereas endogenous viperin was not induced in the stable cells without viral infection (Fig. S6A). We analyzed mitochondrial morphogenesis in cells stably expressing the vector control, the vMIA WT, and the Cys44 vMIA mutant by cellular fractionation. Cell lysates were subjected to subcellular fractionation. Each protein in the mitochondrial and cytosolic fractions was detected by immunoblotting (Fig. S6B). Elongated mitochondria accumulate in the heavy mitochondrial fraction, and fragmented mitochondria accumulate in the light mitochondrial fraction (39). Most mitochondria in these stable cells were found in the heavy mitochondrial fraction. However, mitochondria from cells stably expressing the vMIA WT or the Cys44 vMIA mutant but not the vector control were also found in the light mitochondrial fraction. The presence of light mitochondria was consistent with the small punctate staining observed in cells infected with the recombinant HCMVs (Fig. S5A). The results indicate that mitochondrial fragmentation is induced by the Cys44 vMIA mutant as well as the vMIA WT, confirming that mutation of Cys44 in vMIA does not affect the function of intact vMIA. Next, we used a recombinant HCMV in which vMIA was deleted (HCMV-ΔvMIA) to infect the stable cell lines (Fig. S6C). Consistent with the results of the recombinant HCMV encoding vMIA mutants, the effects of Cys44 of vMIA on the interaction and trafficking of viperin were observed in the stable cell lines infected with HCMV-ΔvMIA (Fig. 6A and B, Fig. S6D). The infectivity of HCMV-ΔvMIA in cells stably expressing the Cys44 vMIA mutant was significantly reduced compared with that in cells stably expressing the vMIA WT (Fig. 6C). However, there was no difference in cell viability between these two stable cell lines infected with HCMV-ΔvMIA (Fig. 6D), indicating that Cys44 of vMIA does not affect the antiapoptotic function of vMIA. In addition, the resultant enhancement of cellular lipogenesis was observed in the stable cell lines infected with HCMV-ΔvMIA (Fig. 6E). Taken together, these results indicate that alterations to the cellular lipid metabolism and viral infectivity that are induced by viperin during HCMV infection can be attributed to Cys44 of vMIA, which is responsible for the interaction and intracellular trafficking of viperin.

DISCUSSION

During human cytomegalovirus (HCMV) infection, viperin plays opposing roles depending on when it is expressed and where it is localized (11). Viperin has antiviral activity in the ER when expressed prior to infection but has proviral activity in the mitochondria during the early stages of infection (9, 10, 20). Viperin is relocalized to the viral AC during late stages of infection, although its function in the AC is unknown. This relocalization suggests that viperin trafficking determines its function during HCMV infection and that some viral or cellular factors are involved in its trafficking and function. At least one viral protein, HCMV vMIA, is responsible for the trafficking of viperin from the ER to the mitochondria during the early stages of infection (9, 10). In the present study, we identified the interaction domains between viperin and vMIA for the first time. We determined that residue Cys44 of vMIA is required for viperin trafficking and clarified its role in the mitochondria during viral replication.

vMIA is an essential protein for viral replication. The two domains (aa 5 to 34 and aa 118 to 147) of vMIA are necessary for its mitochondrial localization and antiapoptotic activity (47). In addition, the acidic domain (aa 81 to 108) of vMIA is required for transactivation of HCMV early gene promoters (48). In the present study, we showed that the residue of vMIA that interacts with viperin is distinct from its functional domains, which suggests that viperin trafficking is independent of the known functions of vMIA.

Viperin is composed of three domains: an N-terminal amphipathic α-helix domain (aa 1 to 42), which is responsible for its association with the cytosolic face of the ER, a

FIG 5 Legend (Continued)

kit. (D) Accumulation of lipid droplets (LDs). Cells were stained with BODIPY 493/503 neutral lipid dye, a marker for LDs, and an antibody specific to HCMV protein IE1 to identify infected cells. A representative image from three independent experiments is shown. Scale bar = 20 μm. (E) Quantification of LDs. The LD number is the mean of 20 cells ± SEM; the LD diameter is the mean of 150 LDs ± SEM. Data are presented as the mean ± SEM of triplicate samples and are representative of three independent experiments. Statistical analysis was performed by one-way ANOVA with Dunnett's multiple-comparison test. *, $P < 0.05$; **, $P < 0.01$; ***, $P < 0.0001$.

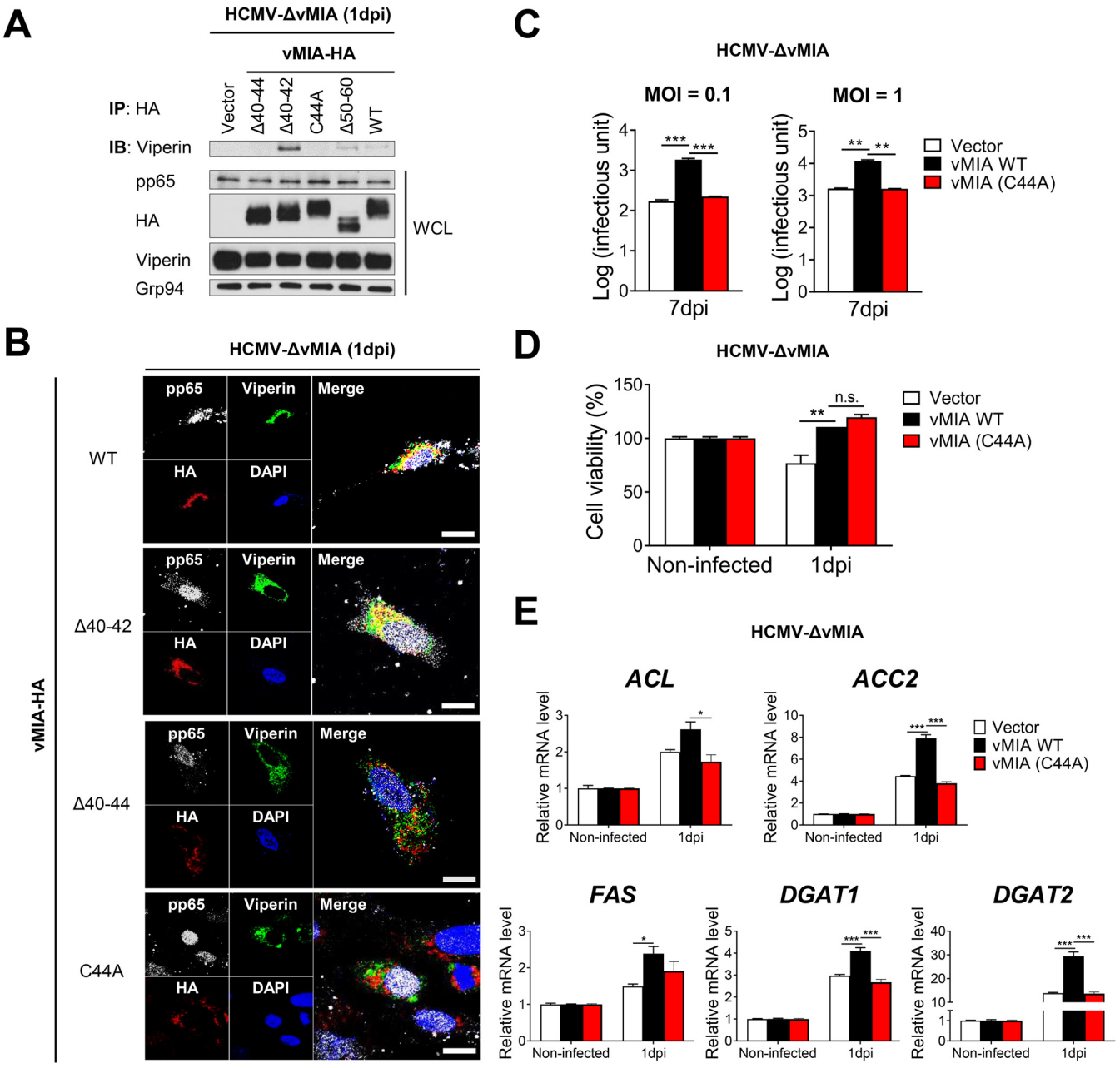

FIG 6 Viperin interaction and trafficking in cells stably expressing vMIA mutants during vMIA-deficient HCMV infection. (A and B) HFtelo cells stably expressing HA-tagged vMIA WT and mutants were infected with an HCMV mutant lacking vMIA (HCMV-ΔvMIA) at an MOI of 1 for 1 day. (A) Viperin interaction with vMIA mutants. Coimmunoprecipitation was performed, and each protein was detected by immunoblotting using specific monoclonal antibodies. HCMV protein pp65 was used as the control for viral protein expression, and Grp94 was used as the loading control. WCL, whole-cell lysate. (B) Intracellular localization of vMIA mutants and endogenous viperin during HCMV-ΔvMIA infection. Cells were stained with antibodies specific to HCMV proteins pp65 and HA-tagged vMIA and viperin. DAPI was used to stain the nuclei. A representative image from two independent experiments is shown. Scale bar = 10 μm. (C and D) HFtelo cells stably expressing vMIA WT and the mutant (C44A) were infected with HCMV-ΔvMIA (C) at an MOI of 0.1 or 1 for 7 days and (D) at an MOI of 1 for 1 day. (C) Viral yield was quantified by a fluorescence-based virus infectivity assay. (D) Cell viability was analyzed by a trypan blue dye-exclusion assay. (E) Relative mRNA levels of lipogenic enzymes in HFtelo cells stably expressing vMIA WT and mutant (C44A) during HCMV-ΔvMIA infection. ACL, ATP-citrate lyase; ACC2, acetyl-coenzyme A (CoA) carboxylase 2; FAS, fatty acid synthase; DGAT1 and DGAT2, diacylglycerol acyltransferases 1 and 2. Data are presented as the mean ± SEM of triplicate samples and are representative of three independent experiments. Statistical analysis was performed by one-way ANOVA with Dunnett's multiple-comparison test. *, $P < 0.05$; **, $P < 0.01$; ***, $P < 0.0001$.

central domain (aa 71 to 182), in which the Fe-S cluster binding motif is essential for its functional activities, and a C-terminal domain (aa 183 to 361), which is highly conserved but functionally undefined (11). The Fe-S cluster binding motif of viperin is required for its ability to alter lipid metabolism during HCMV infection (9, 10). We found that the N-terminal domain of viperin is necessary for its interaction with vMIA.

Moreover, we demonstrated that the structure, rather than the sequence composition, of the N-terminal domain of viperin is required for its interaction with vMIA by proving that the N-terminal domain of mouse viperin, which is structurally similar to that of human viperin, interacts with vMIA. Human and mouse viperin have similar motifs and amino acid residues, although they are not identical. The N-terminal domain of human and mouse viperin contains a leucine zipper motif (aa 14 to 42), which is typically hydrophobic (11, 21). This motif is responsible for the binding of viperin to the intracellular membrane by enhancing the electrostatic interactions in protein-protein bonds (21, 49). It has been suggested that the N-terminal domain of viperin might be required for the electrostatic interaction with vMIA. Human and mouse viperin also both have a cysteine residue (Cys33) within the N-terminal domain. However, Cys33 of viperin was not required for the interaction with Cys44 of vMIA, indicating that the interaction between viperin and vMIA is not caused by forming a disulfide bond between cysteine residues. Expression of mouse viperin rescues the HCMV WT phenotype in terms of viral replication in human viperin knockdown cells (9). Our data suggest that the N-terminal domain of mouse viperin can functionally replace that of human viperin during HCMV infection, although the structural mechanism by which vMIA interacts with viperin needs to be further elucidated.

A three-dimensional model has been generated of the interaction between vMIA and the apoptosis regulator Bax based on their sequence-to-structure alignment. vMIA recruits Bax to the mitochondria and triggers the oligomerization of Bax by establishing multivalent and/or cooperative interactions with Bax (30, 31). Similar to the vMIA-Bax interaction, the vMIA interaction with the N terminus of viperin might affect the oligomerization of viperin as well as its targeting to the mitochondria.

We generated a series of recombinant HCMVs to analyze the effect of vMIA Cys44 on the interaction with viperin during viral infection. vMIA is also known as pUL37x1. The immediate early gene of HCMV, *UL37*, produces an unspliced transcript encoding pUL37x1 and two spliced transcripts encoding gpUL37 and gpUL37M (22, 23, 50). In the present study, the HA-tagged recombinant HCMVs, in which the HA-tag sequence was inserted between the alternative splicing site and the stop codon of vMIA (UL37x1), encode the HA-tag for vMIA, but not gpUL37 or gpUL37M. The expression levels of other viral proteins, IE1 and pp65, were not altered in cells infected with the recombinant viruses compared with cells infected with HCMV WT. Therefore, our strategy was appropriate to verify the effect of vMIA on the interaction with viperin during viral infection.

Many cellular and viral proteins temporally alter their subcellular localization during HCMV infection. Various proteins, such as the ER-Golgi intermediate compartment (ERGIC) marker proteins (51), lysosomal marker proteins, soluble N-ethylmaleimide-sensitive factor attachment protein receptor (SNARE) family members (52, 53), and endosomal sorting complex required for transport (ESCRT) components (54, 55), as well as several viral proteins, including gB and pp65, localize to the AC during the late stages of infection. Viperin also localizes to the AC during the late stages of infection, although vMIA remains associated with the mitochondria. This suggests that viperin moves from the mitochondria to the AC, or directly from the ER to the AC, by interacting with cellular or viral proteins other than vMIA. In the present study we showed that the efficiency of viperin trafficking to the AC was remarkably reduced in cells infected with the recombinant HCMV encoding the Cys44 vMIA mutant compared with cells infected with the HCMV WT. This indicates that viperin mainly migrates to the AC via the mitochondria, rather than directly from the ER, although a small amount of viperin is still observed in the AC of cells infected with the recombinant HCMV encoding the vMIA Cys44 mutant. Therefore, we hypothesize that viperin traffics from the ER to the AC via the mitochondria during HCMV infection. The mitochondrial localization of viperin is a prerequisite for AC localization. In summary, viperin's interaction with vMIA is essential for its trafficking to the mitochondria, and Cys44 of vMIA is also crucial for the trafficking of viperin.

Failure of viperin to localize to the mitochondria results in insufficient lipogenesis and thus reduces viral replication (10), The mitochondrial localization of the viperin mutant lacking the Fe-S cluster binding motif is similarly impaired (10). Consistent with these data,

we found that the mislocalization of viperin in cells infected with the recombinant HCMV encoding the Cys44 vMIA mutant produces defects in cellular lipogenesis and viral replication. Our data indicate that the function of viperin is determined by its localization during viral infection, although the domain of viperin that is responsible for its interaction with vMIA is distinct from the domain that exerts its other functions. Altogether, the interacting domains of vMIA and viperin are required for the trafficking and function of viperin that result in enhanced viral replication.

In conclusion, we demonstrated that Cys44 of vMIA is a critical amino acid for viperin trafficking during HCMV replication. The multiple roles of viperin, which depend on its localization, during viral infection are primarily dependent on a single amino acid of the HCMV protein vMIA. Our findings suggest that this may be a potential therapeutic target for HCMV-associated diseases.

MATERIALS AND METHODS

Cells, viruses, antibodies, and reagents. HeLa, COS-7, and HEK 293T cells were used for transient transfection experiments. Human foreskin fibroblast (HFF) and telomerase-immortalized human fibroblast (HFtelo) cells were kindly provided by P. Cresswell (Yale University). All cells were cultured and maintained in Dulbecco's modified Eagle's medium (DMEM) supplemented with 10% fetal bovine serum (FBS) (HyClone) and 1% penicillin-streptomycin (HyClone) at 37°C in a 5% CO_2 incubator.

The bacterial artificial chromosome (BAC) pHB15 containing HCMV strain AD169 was kindly provided by T. Stamminger (Ulm University Medical Center) (42), and the recombination system using rpsL-neo selection was provided by J. H. Ahn (Sungkyunkwan University) (56). The recombinant HCMVs used in the present study were generated utilizing a recombination strategy in HCMV (AD169)-BAC. Recombinant BACs were reconstituted to viruses by transfecting BAC DNA into HFFs with a Nucleofector kit (Lonza) according to the manufacturer's instructions. Cells infected with the recombinant viruses were harvested, and viral DNA was isolated using a QIAamp DNA minikit (Qiagen). Nucleotide sequence analysis of PCR products amplified from viral DNA was used to confirm that the recombinant viruses contained the desired mutations. HCMV strain RVHB5 WT and HCMV RVHB5 ΔvMIA mutants were kindly provided by E. S. Mocarski (Emory University) (57).

HCMV-encoded proteins were detected with specific monoclonal antibodies (MAb). The mouse MAb to vMIA (4B6-B) was a gift from T. Shenk (Princeton University). The mouse MAbs to IE-1 (UL123) (P63-27) and pp65 (UL83) (28-19) were gifts from W. J. Britt (University of Alabama at Birmingham). The mouse MAb to viperin (MaP.VIP) was provided by P. Cresswell (Yale University) (14, 20). The mouse MAbs to Myc (4A6) (Merk Millipore), mtHSP70 (JG1) (Abcam), and α-tubulin (DM1A) (Sigma-Aldrich), the rabbit MAbs to hemagglutinin (HA) and calnexin (Abcam), and the rat MAb to Grp94 (Enzo Life Sciences) were purchased from their respective suppliers. Goat anti-rabbit, anti-mouse, and anti-rat IgG secondary antibodies (Abs) were purchased from Jackson ImmunoResearch Laboratories. Normal rabbit serum (NRS) and normal mouse serum (NMS) were also used as negative controls. Mitotracker Red (Invitrogen), BODIPY 493/503 neutral lipid dye (Molecular Probes), Lipofectamine 2000 (Thermo Fisher Scientific), Polybrene (Merk Millipore), and G418 (Duchefa Biochemie) were purchased from their respective suppliers.

Bacmid mutagenesis. The HCMV (AD169)-BAC clone was used as the template for mutagenesis. HCMV (AD169)-BAC clones containing UL37x1 (vMIA) mutations were generated using a counter-selection BAC modification kit (Gene Bridges) according to the manufacturer's instructions. Briefly, the rpsL-neo cassette, together with 50 nucleotides of the AD169 sequence flanking the target region within the HCMV genome, was generated by PCR amplification using the primer set (rpsL-neo-set1) listed in Table S1. The rpsL-neo cassette with homology arms was introduced into *E. coli* DH10B containing HCMV (AD169)-BAC by electroporation using a Gene Pulser II (Bio-Rad). HCMV (AD169)-BAC clones with homologous recombination of the rpsL-neo cassette were selected on LB plates containing kanamycin (Sigma-Aldrich). Thereafter, the rpsL-neo cassette was replaced by annealed oligonucleotide DNAs consisting of vMIA mutations with homology arms of 50 nucleotides. The primer set for PCR amplification of vMIA mutants is listed in Table S1. HCMV (AD169)-BAC clones with homologous recombination of vMIA mutants were selected on LB plates containing streptomycin (Sigma-Aldrich). HCMV (AD169)-BACs encoding HA-tagged vMIA mutants were then generated from the recombinant HCMV (AD169)-BACs encoding vMIA mutants. The rps-neo cassette flanked by homology arms was reinserted into the target region of the recombinant HCMV (AD169)-BACs. Thereafter, the rpsL-neo cassette was replaced by the DNA fragments containing HA-tagged vMIA mutants with homology arms by recombination. The HA-tag sequence was added after nucleotide 489 of vMIA, which is a splice site for UL37. The primer set (rpsL-neo-set2) for PCR amplification of this rps-neo cassette and the vMIA-HA primer set are also listed in Table S1. Revertant HCMV (AD169)-BACs were also generated from the recombinant HCMV-BACs encoding vMIA mutants as described above. The target regions of the recombinant HCMV-BACs were amplified by PCR and sequenced to verify the desired mutations.

Plasmids and transfections. Human and mouse viperin cDNA constructs of the wild type (WT), truncation of residues 1 to 42 or 1 to 80, deletion of residues 2 to 42 (Δ2 to 42), and substitution of cysteine residue 33 to alanine residue (C33A) were generated by PCR amplification and were then cloned into pcDNA3.1 with a C-terminal HA-tag or 6Myc-tag. The coding region for vMIA (UL37x1) was produced by PCR from genomic HCMV (strain AD169) DNA. vMIA cDNA constructs of the WT, a series of truncation mutants (1 to 22, 1 to 34, 1 to 39, 1 to 44, 1 to 49, 1 to 54, or 1 to 60), deletion mutants (Δ2 to 34, Δ2 to 22, Δ35 to 39, Δ40 to 44, Δ40 to 42, Δ45 to 49, or Δ50 to 60), and substitution mutants (C44A, K40A, K41A, K42A, KK4041AA, KK4142AA,

KK4042AA, or KKK404142AAA) were generated by PCR amplification, and were then cloned into pcDNA3.1 with a C-terminal HA-tag or 6Myc-tag. Ribosomal protein subunit 14 (Rps14), a negative control, was amplified by PCR and cloned into pcDNA3.1 with a C-terminal HA-tag or 6Myc-tag. pBMN-Z-IRES-Neo plasmid and pCL-Ampho plasmid were kindly provided by Peter Cresswell (Yale University). Constructs were transfected into HFFs using a Nucleofector kit (Lonza) according to the manufacturer's instructions or HEK 293T, HeLa, and COS-7 cells using Lipofectamine 2000 (Thermo Fisher Scientific), according to the manufacturer's instructions.

Stable cell lines. HEK 293T cells were cotransfected with two plasmids: 12 μg of pBMN-vMIA-IRES-Neo plasmid and 12 μg of pCL-Ampho plasmid, using Lipofectamine 2000. The cotransfected cells were incubated at 37°C for 8 h and then transferred to 32°C. After 1 day, the supernatant containing lentiviruses was collected every 24 h three times. HFtelo cells were spin-infected with the supernatants containing viruses for 90 min (2,500 rpm) at 32°C in the presence of Polybrene (8 μg/mL) three times and incubated at 32°C. After 1 day, the infected cells were transferred to 37°C and selected with neomycin (1 mg/mL). Protein expression efficiency was assessed by Western blot analysis from cells stably expressing the indicated vMIA mutants.

Immunoblot analysis. Cells were harvested and lysed with 1% Triton X-100 in Tris-buffered saline (TBS) containing proteinase inhibitors. The supernatants of the lysates were collected, and the concentration of protein was determined by bicinchoninic acid (BCA) assay (Thermo Fisher Scientific). The proteins were separated electrophoretically on 12% SDS-PAGE gels and transferred to polyvinylidene fluoride (PVDF) membranes (Merk Millipore). The blots were blocked with 5% skim milk and 0.05% Tween in phosphate-buffered saline (PBS), incubated with primary antibodies, and probed with horseradish peroxidase-conjugated secondary antibodies, followed by incubation with enhanced chemiluminescence reagent (Thermo Fisher Scientific). Grp94 was used as the loading control.

Coimmunoprecipitation. HEK 293T cells were seeded on 60-mm dishes (SPL Life Sciences) and cotransfected with the indicated plasmids. Cells were harvested 24 h after transfection, washed three times with PBS, and lysed with 1% Brij 98 (Sigma-Aldrich) in TBS for 1 h at 4°C. The cell lysates were precleared with normal mouse or rabbit serum and protein G or A Sepharose (GE Healthcare) for 1 h at 4°C. The precleared lysates were immunoprecipitated by incubation with specific antibodies and protein G or A Sepharose for 1 h at 4°C. Immunoprecipitates were rinsed three times with 0.1% Brij 98 in TBS, eluted in reducing sample buffer, electrophoresed on 12% SDS-PAGE gels, and then blotted with specific antibodies. HFFs or HFtelo cells stably expressing vMIA WT and mutants were seeded on 10- mm dishes (SPL Life Sciences) and infected with the recombinant HCMVs at a multiplicity of infection (MOI) of 1 for 24 h. Cells were harvested at the indicated time and lysed. The cell lysates were immunoprecipitated as described above.

Immunofluorescence. HFFs and HFtelo cells stably expressing vMIA WT and mutants were grown in 24-well tissue culture plates (SPL Life Sciences) containing a 13-mm-diameter coverslip. After the cells reached 80 to 90% confluence, they were infected with recombinant HCMVs at an MOI of 1 for the indicated times. The coverslips were harvested by washing the cells with PBS and then fixing cells with 3% paraformaldehyde (Sigma-Aldrich) in PBS for 45 min at room temperature. The coverslips were washed with PBS and permeabilized with 0.1% Triton X-100 and 0.01% SDS in PBS for 7 min. The coverslips were then blocked with 0.2% Tween in PBS containing 10% normal goat serum (Thermo Fisher Scientific) for 20 min at room temperature, followed by the addition of primary antibodies, and then incubated for 1 h at room temperature. The coverslips were washed with 0.2% Tween in PBS and incubated with anti-mouse IgG secondary antibodies (Thermo Fisher Scientific) for 45 min at room temperature. The coverslips were washed with 0.2% Tween in PBS, rinsed once in PBS, and mounted with ProLong Gold antifade reagent (Molecular Probes). Images were acquired with a LSM700 scanning laser confocal microscope (Carl Zeiss AG) and analyzed using Zeiss ZEN 2012 software and ImageJ software. Lipid droplets (LDs) were monitored by immunofluorescence. HFFs were grown on coverslips and infected with recombinant HCMVs at an MOI of 1 for 3 days. The coverslips were fixed and permeabilized with 0.5% saponin in PBS for 10 min. The coverslips were then incubated with the indicated antibodies followed by the addition of 10 μg/mL BODIPY 493/503 neutral lipid dye in 150 mM NaCl for 20 min at room temperature. HeLa and COS-7 cells grown on the coverslips were transfected with the indicated plasmids. After 24 h, the coverslips were fixed and stained with specific antibodies as described above. To visualize mitochondria, cells were incubated with Mitotracker Red before fixation.

Subcellular fractionation. Cells were fractionated to isolate heavy mitochondrial fractions, light mitochondrial fractions, and cytosolic fractions as described previously (38, 39). Briefly, cells were collected, resuspended in 1 mL of homogenization buffer (0.25 M sucrose, 10 mM HEPES-NaOH [pH 7.4], and 1 mM EDTA) supplemented with protease inhibitor cocktail (Roche), and then placed on ice for 10 min. Cells were broken by needle passage (15 to 20 passages through 25-gauge needles), followed by centrifugation at 1,000 $\times$ *g* for 10 min at 4°C to remove nuclei and unbroken cells. The supernatant was subsequently centrifuged at 3,000 $\times$ *g* for 10 min at 4°C, and the pellet was used as a heavy mitochondrial fraction. The supernatant was further centrifuged at 17,000 $\times$ *g* for 10 min at 4°C, and the pellet was used as a light mitochondrial fraction. The supernatant was separated by ultracentrifugation at 65,000 $\times$ *g* for 60 min at 4°C to eliminate microsomes (pellet) from cytosol (supernatant). The purified mitochondrial pellets were washed twice in PBS and suspended in SDS-PAGE sample buffer until assay.

RNA extraction, cDNA preparation, and quantitative real-time PCR. Cells were collected, and total RNA was extracted using a cultured cell total RNA purification kit (Favorgen). The cDNA was synthesized from 1 μg RNA template using a PrimeScript RT reagent kit according to the manufacturer's instructions (TaKaRa Bio). The cDNA was quantified by quantitative real-time PCR (qRT-PCR) using a TB Green fast qPCR reagent kit (TaKaRa Bio). The primers used for PCR are listed in Table S2. The PCR was performed in triplicate for each sample. Quantitation was performed using the comparative threshold cycle (C_T) ($2^{-\Delta\Delta CT}$) method. The C_T value for target genes in each sample was normalized to that of β-actin. Three independent experiments were analyzed to determine differences in the mean values, and *P* values are indicated in the figures.

Measurement of neutral lipids. Cells were grown on 100-mm dishes (SPL Life Sciences) and then infected with recombinant HCMVs at an MOI of 1 for 3 days. The cells were counted and lysed in 0.3 mL of Triton X-100 (0.5% in H_2O). Neutral lipids were extracted by sequentially adding 0.75 mL of methanol, 0.75 mL of chloroform, 0.75 mL of chloroform, and 0.75 mL of H_2O, with vortexing. Samples were centrifuged at 3,000 $\times$ *g* for 15 min at room temperature, and the organic phase (lower phase) was recovered. The amount of neutral lipids was measured with a lipid assay kit (Abcam ab242307) according to the manufacturer's instructions. In brief, samples and neutral lipid standards were added into a black, clear-bottom microplate (SPL Life Sciences) and incubated at 55°C for 30 min. The plate was cooled for 3 min at 4°C, followed by the addition of isopropanol, and then incubated for 5 min at room temperature. Fluorometric reagent was added, and fluorescence was measured as excitation/emission (Ex/Em) = 490 nm/585 nm. The fluorescence intensity expressed as relative fluorescence units (RFU) was converted into the lipid concentration using lipid standard solutions. The data sets were analyzed statistically for differences in the mean values, and *P* values are indicated in the figures.

Cell viability assay. HFtelo cells stably expressing vMIA WT and mutants were grown in 6-well tissue culture plates (7×10^5 cells/well) (SPL Life Sciences). The cells were infected with RVHB5 lacking vMIA (ΔvMIA-HCMV) at an MOI of 1 for 1 day. The cells were washed with PBS, trypsinized with 0.25% trypsin-EDTA (HyClone), and resuspended in the culture medium. The cells were then pelleted by centrifugation, resuspended in 1 mL of fresh culture medium, and stained with trypan blue (Thermo Fisher Scientific). Cell viability was determined by counting the number of live and dead cells under a phase-contrast microscope. The assay was performed in duplicate for each sample.

Annexin V/propidium iodide (PI) apoptosis assay. HFFs were seeded on 60-mm dishes (2×10^6 cells/dish) (SPL Life Sciences) and incubated overnight in 5% CO_2 at 37°C. Cells were infected with recombinant HCMVs at an MOI of 2 for 3 or 5 days. Supernatants and cells were harvested and then washed twice in cold PBS. Apoptotic cells were identified by incubation in 100 μL Annexin V binding buffer containing 200 μg/mL of Alexa Fluor 647-conjugated Annexin V and 1 μg/mL of PI for 15 min in the dark at room temperature. Cells were examined using a BD FACS Verse II flow cytometer (Becton, Dickinson). In total, 10,000 cells were analyzed per measurement. Untreated cells were used as a negative control. Data were analyzed using FlowJo 10.0.7 software (Tree Star, Inc., Ashland, OR, USA). Three independent experiments were analyzed statistically for differences in the mean values, and the *P* values are indicated in the figures.

Virus replication assay. HFFs were infected with recombinant HCMVs at an MOI of 0.05 for 2 h and then washed and cultured in DMEM supplemented with 10% FBS and 1% penicillin-streptomycin. Supernatants and cells were harvested at 1, 3, 5, and 7 dpi. Viral yield was measured by performing a fluorescence-based viral infectivity assay (58). HFtelo cells stably expressing vMIA WT and mutants (C44A) were infected with RVHB5 lacking vMIA (ΔvMIA-HCMV) at an MOI of 0.1 or 1 for 2 h. Viral yield was then assayed as described above.

Statistical analysis. The data are presented as the mean $\pm$ standard error of the mean (SEM). Statistical significance was determined using one-way analysis of variance (ANOVA) with Dunnett's multiple-comparison test. *P* values of <0.05 were considered statistically significant.

Data availability. All relevant data are within the manuscript and its supplemental material files.

SUPPLEMENTAL MATERIAL

Supplemental material is available online only.

SUPPLEMENTAL FILE 1, PDF file, 1.6 MB.

ACKNOWLEDGMENTS

This study was supported by grants from the National Research Foundation of Korea (NRF) funded by the Ministry of Science and ICT (NRF-2021R1A2C1011092, NRF-2021M3A9I2080496, and NRF-2022M3A9I2017587) and a faculty research grant from Yonsei University College of Medicine for 2020 (6-2020-0230) to J.-Y. Seo and Graduate School of Medical Science, Brain Korea 21 Project, Yonsei University College of Medicine.

J.-Y.S. conceived and designed experiments. J.J.K. and S.H. performed experiments. J.J.K. and J.-Y.S. analyzed and interpreted the data. J.J.K. and J.-Y.S. wrote the manuscript. All authors contributed to the final version of the manuscript.

We declare that no competing interests exists.

REFERENCES

1. Fülöp T, Larbi A, Pawelec G. 2013. Human T cell aging and the impact of persistent viral infections. Front Immunol 4:271–271. https://doi.org/10.3389/fimmu.2013.00271.
2. Meakins JL. 1983. Clinical approach to infection in the compromised host. Ann Surg 197:491–491.
3. Landolfo S, Gariglio M, Gribaudo G, Lembo D. 2003. The human cytomegalovirus. Pharmacol Ther 98:269–297. https://doi.org/10.1016/s0163-7258(03)00034-2.
4. Warnatsch A. 2013. Impact of proteasomal immune adaptation on the early immune response to viral infection. PhD thesis. Kings College London, London, UK.
5. Crough T, Khanna R. 2009. Immunobiology of human cytomegalovirus: from bench to bedside. Clin Microbiol Rev 22:76–98. https://doi.org/10.1128/CMR.00034-08.
6. Munger J, Bajad SU, Coller HA, Shenk T, Rabinowitz JD. 2006. Dynamics of the cellular metabolome during human cytomegalovirus infection. PLoS Pathog 2:e132. https://doi.org/10.1371/journal.ppat.0020132.
7. Vastag L, Koyuncu E, Grady SL, Shenk TE, Rabinowitz JD. 2011. Divergent effects of human cytomegalovirus and herpes simplex virus-1 on cellular metabolism. PLoS Pathog 7:e1002124. https://doi.org/10.1371/journal.ppat.1002124.
8. Munger J, Bennett BD, Parikh A, Feng XJ, McArdle J, Rabitz HA, Shenk T, Rabinowitz JD. 2008. Systems-level metabolic flux profiling identifies fatty

acid synthesis as a target for antiviral therapy. Nat Biotechnol 26:1179–1186. https://doi.org/10.1038/nbt.1500.
9. Seo JY, Yaneva R, Hinson ER, Cresswell P. 2011. Human cytomegalovirus directly induces the antiviral protein viperin to enhance infectivity. Science 332:1093–1097. https://doi.org/10.1126/science.1202007.
10. Seo JY, Cresswell P. 2013. Viperin regulates cellular lipid metabolism during human cytomegalovirus infection. PLoS Pathog 9:e1003497. https://doi.org/10.1371/journal.ppat.1003497.
11. Seo JY, Yaneva R, Cresswell P. 2011. Viperin: a multifunctional, interferon-inducible protein that regulates virus replication. Cell Host Microbe 10:534–539. https://doi.org/10.1016/j.chom.2011.11.004.
12. Jiang D, Guo H, Xu C, Chang J, Gu B, Wang L, Block TM, Guo JT. 2008. Identification of three interferon-inducible cellular enzymes that inhibit the replication of hepatitis C virus. J Virol 82:1665–1678. https://doi.org/10.1128/JVI.02113-07.
13. Rivieccio MA, Suh HS, Zhao Y, Zhao ML, Chin KC, Lee SC, Brosnan CF. 2006. TLR3 ligation activates an antiviral response in human fetal astrocytes: a role for viperin/cig5. J Immunol 177:4735–4741. https://doi.org/10.4049/jimmunol.177.7.4735.
14. Wang X, Hinson ER, Cresswell P. 2007. The interferon-inducible protein viperin inhibits influenza virus release by perturbing lipid rafts. Cell Host Microbe 2:96–105. https://doi.org/10.1016/j.chom.2007.06.009.
15. Zhang Y, Burke CW, Ryman KD, Klimstra WB. 2007. Identification and characterization of interferon-induced proteins that inhibit alphavirus replication. J Virol 81:11246–11255. https://doi.org/10.1128/JVI.01282-07.
16. Eom J, Kim JJ, Yoon SG, Jeong H, Son S, Lee JB, Yoo J, Seo HJ, Cho Y, Kim KS, Choi KM, Kim IY, Lee HY, Nam KT, Cresswell P, Seong JK, Seo JY. 2019. Intrinsic expression of viperin regulates thermogenesis in adipose tissues. Proc Natl Acad Sci U S A 116:17419–17428. https://doi.org/10.1073/pnas.1904480116.
17. Saitoh T, Satoh T, Yamamoto N, Uematsu S, Takeuchi O, Kawai T, Akira S. 2011. Antiviral protein viperin promotes Toll-like receptor 7- and Toll-like receptor 9-mediated type I interferon production in plasmacytoid dendritic cells. Immunity 34:352–363. https://doi.org/10.1016/j.immuni.2011.03.010.
18. Kim JJ, Kim KS, Eom J, Lee JB, Seo JY. 2019. Viperin differentially induces interferon-stimulated genes in distinct cell types. Immune Netw 19:e33. https://doi.org/10.4110/in.2019.19.e33.
19. Eom J, Yoo J, Kim JJ, Lee JB, Choi W, Park CG, Seo JY. 2018. Viperin deficiency promotes polarization of macrophages and secretion of M1 and M2 cytokines. Immune Netw 18:e32. https://doi.org/10.4110/in.2018.18.e32.
20. Chin KC, Cresswell P. 2001. Viperin (cig5), an IFN-inducible antiviral protein directly induced by human cytomegalovirus. Proc Natl Acad Sci U S A 98:15125–15130. https://doi.org/10.1073/pnas.011593298.
21. Hinson ER, Cresswell P. 2009. The N-terminal amphipathic alpha-helix of viperin mediates localization to the cytosolic face of the endoplasmic reticulum and inhibits protein secretion. J Biol Chem 284:4705–4712. https://doi.org/10.1074/jbc.M807261200.
22. Goldmacher VS, Bartle LM, Skaletskaya A, Dionne CA, Kedersha NL, Vater CA, Han JW, Lutz RJ, Watanabe S, Cahir McFarland ED, Kieff ED, Mocarski ES, Chittenden T. 1999. A cytomegalovirus-encoded mitochondria-localized inhibitor of apoptosis structurally unrelated to Bcl-2. Proc Natl Acad Sci U S A 96:12536–12541. https://doi.org/10.1073/pnas.96.22.12536.
23. McCormick AL, Skaletskaya A, Barry PA, Mocarski ES, Goldmacher VS. 2003. Differential function and expression of the viral inhibitor of caspase 8-induced apoptosis (vICA) and the viral mitochondria-localized inhibitor of apoptosis (vMIA) cell death suppressors conserved in primate and rodent cytomegaloviruses. Virology 316:221–233. https://doi.org/10.1016/j.virol.2003.07.003.
24. Mavinakere MS, Colberg-Poley AM. 2004. Dual targeting of the human cytomegalovirus UL37 exon 1 protein during permissive infection. J Gen Virol 85:323–329. https://doi.org/10.1099/vir.0.19589-0.
25. Mavinakere MS, Williamson CD, Goldmacher VS, Colberg-Poley AM. 2006. Processing of human cytomegalovirus UL37 mutant glycoproteins in the endoplasmic reticulum lumen prior to mitochondrial importation. J Virol 80:6771–6783. https://doi.org/10.1128/JVI.00492-06.
26. Williamson CD, Colberg-Poley AM. 2010. Intracellular sorting signals for sequential trafficking of human cytomegalovirus UL37 proteins to the endoplasmic reticulum and mitochondria. J Virol 84:6400–6409. https://doi.org/10.1128/JVI.00556-10.
27. Norris KL, Youle RJ. 2008. Cytomegalovirus proteins vMIA and m38.5 link mitochondrial morphogenesis to Bcl-2 family proteins. J Virol 82:6232–6243. https://doi.org/10.1128/JVI.02710-07.
28. Arnoult D, Bartle LM, Skaletskaya A, Poncet D, Zamzami N, Park PU, Sharpe J, Youle RJ, Goldmacher VS. 2004. Cytomegalovirus cell death suppressor vMIA blocks Bax- but not Bak-mediated apoptosis by binding and sequestering Bax at mitochondria. Proc Natl Acad Sci U S A 101:7988–7993. https://doi.org/10.1073/pnas.0401897101.
29. Poncet D, Larochette N, Pauleau AL, Boya P, Jalil AA, Cartron PF, Vallette F, Schnebelen C, Bartle LM, Skaletskaya A, Boutolleau D, Martinou JC, Goldmacher VS, Kroemer G, Zamzami N. 2004. An anti-apoptotic viral protein that recruits Bax to mitochondria. J Biol Chem 279:22605–22614. https://doi.org/10.1074/jbc.M308408200.
30. Ma J, Edlich F, Bermejo GA, Norris KL, Youle RJ, Tjandra N. 2012. Structural mechanism of Bax inhibition by cytomegalovirus protein vMIA. Proc Natl Acad Sci U S A 109:20901–20906. https://doi.org/10.1073/pnas.1217094110.
31. Pauleau AL, Larochette N, Giordanetto F, Scholz SR, Poncet D, Zamzami N, Goldmacher VS, Kroemer G. 2007. Structure-function analysis of the interaction between Bax and the cytomegalovirus-encoded protein vMIA. Oncogene 26:7067–7080. https://doi.org/10.1038/sj.onc.1210511.
32. Poncet D, Pauleau AL, Szabadkai G, Vozza A, Scholz SR, Le Bras M, Briere JJ, Jalil A, Le Moigne R, Brenner C, Hahn G, Wittig I, Schagger H, Lemaire C, Bianchi K, Souquere S, Pierron G, Rustin P, Goldmacher VS, Rizzuto R, Palmieri F, Kroemer G. 2006. Cytopathic effects of the cytomegalovirus-encoded apoptosis inhibitory protein vMIA. J Cell Biol 174:985–996. https://doi.org/10.1083/jcb.200604069.
33. Magalhães AC, Ferreira AR, Gomes S, Vieira M, Gouveia A, Valenca I, Islinger M, Nascimento R, Schrader M, Kagan JC, Ribeiro D. 2016. Peroxisomes are platforms for cytomegalovirus' evasion from the cellular immune response. Sci Rep 6:26028. https://doi.org/10.1038/srep26028.
34. Hell R, Wirtz M. 2011. Molecular biology, biochemistry and cellular physiology of cysteine metabolism in Arabidopsis thaliana. Arabidopsis Book 9:e0154. https://doi.org/10.1199/tab.0154.
35. Meitzler JL, Hinde S, Banfi B, Nauseef WM, Ortiz de Montellano PR. 2013. Conserved cysteine residues provide a protein-protein interaction surface in dual oxidase (DUOX) proteins. J Biol Chem 288:7147–7157. https://doi.org/10.1074/jbc.M112.414797.
36. Sokalingam S, Raghunathan G, Soundrarajan N, Lee SG. 2012. A study on the effect of surface lysine to arginine mutagenesis on protein stability and structure using green fluorescent protein. PLoS One 7:e40410. https://doi.org/10.1371/journal.pone.0040410.
37. Wu X, Knudsen B, Feller SM, Zheng J, Sali A, Cowburn D, Hanafusa H, Kuriyan J. 1995. Structural basis for the specific interaction of lysine-containing proline-rich peptides with the N-terminal SH3 domain of c-Crk. Structure 3:215–226. https://doi.org/10.1016/s0969-2126(01)00151-4.
38. Zhyvoloup A, Nemazanyy I, Panasyuk G, Valovka T, Fenton T, Rebholz H, Wang ML, Foxon R, Lyzogubov V, Usenko V, Kyyamova R, Gorbenko O, Matsuka G, Filonenko V, Gout IT. 2003. Subcellular localization and regulation of coenzyme A synthase. J Biol Chem 278:50316–50321. https://doi.org/10.1074/jbc.M307763200.
39. McCormick AL, Smith VL, Chow D, Mocarski ES. 2003. Disruption of mitochondrial networks by the human cytomegalovirus UL37 gene product viral mitochondrion-localized inhibitor of apoptosis. J Virol 77:631–641. https://doi.org/10.1128/jvi.77.1.631-641.2003.
40. Chakravarti A, Selvadurai K, Shahoei R, Lee H, Fatma S, Tajkhorshid E, Huang RH. 2018. Reconstitution and substrate specificity for isopentenyl pyrophosphate of the antiviral radical SAM enzyme viperin. J Biol Chem 293:14122–14133. https://doi.org/10.1074/jbc.RA118.003998.
41. Fenwick MK, Li Y, Cresswell P, Modis Y, Ealick SE. 2017. Structural studies of viperin, an antiviral radical SAM enzyme. Proc Natl Acad Sci U S A 114:6806–6811. https://doi.org/10.1073/pnas.1705402114.
42. Lorz K, Hofmann H, Berndt A, Tavalai N, Mueller R, Schlotzer-Schrehardt U, Stamminger T. 2006. Deletion of open reading frame UL26 from the human cytomegalovirus genome results in reduced viral growth, which involves impaired stability of viral particles. J Virol 80:5423–5434. https://doi.org/10.1128/JVI.02585-05.
43. Spencer CM, Schafer XL, Moorman NJ, Munger J. 2011. Human cytomegalovirus induces the activity and expression of acetyl-coenzyme A carboxylase, a fatty acid biosynthetic enzyme whose inhibition attenuates viral replication. J Virol 85:5814–5824. https://doi.org/10.1128/JVI.02630-10.
44. Yu Y, Maguire TG, Alwine JC. 2012. Human cytomegalovirus infection induces adipocyte-like lipogenesis through activation of sterol regulatory element binding protein 1. J Virol 86:2942–2949. https://doi.org/10.1128/JVI.06467-11.
45. Farese RV Jr, Walther TC. 2009. Lipid droplets finally get a little R-E-S-P-E-C-T. Cell 139:855–860. https://doi.org/10.1016/j.cell.2009.11.005.

46. Guo Y, Cordes KR, Farese RV Jr, Walther TC. 2009. Lipid droplets at a glance. J Cell Sci 122:749–752. https://doi.org/10.1242/jcs.037630.
47. Hayajneh WA, Colberg-Poley AM, Skaletskaya A, Bartle LM, Lesperance MM, Contopoulos-Ioannidis DG, Kedersha NL, Goldmacher VS. 2001. The sequence and antiapoptotic functional domains of the human cytomegalovirus UL37 exon 1 immediate early protein are conserved in multiple primary strains. Virology 279:233–240. https://doi.org/10.1006/viro.2000.0726.
48. Colberg-Poley AM, Huang L, Soltero VE, Iskenderian AC, Schumacher RF, Anders DG. 1998. The acidic domain of pUL37x1 and gpUL37 plays a key role in transactivation of HCMV DNA replication gene promoter constructions. Virology 246:400–408. https://doi.org/10.1006/viro.1998.9212.
49. Hendsch ZS, Tidor B. 1999. Electrostatic interactions in the GCN4 leucine zipper: substantial contributions arise from intramolecular interactions enhanced on binding. Protein Sci 8:1381–1392. https://doi.org/10.1110/ps.8.7.1381.
50. Goldmacher VS. 2002. vMIA, a viral inhibitor of apoptosis targeting mitochondria. Biochimie 84:177–185. https://doi.org/10.1016/s0300-9084(02)01367-6.
51. Tandon R, Mocarski ES. 2012. Viral and host control of cytomegalovirus maturation. Trends Microbiol 20:392–401. https://doi.org/10.1016/j.tim.2012.04.008.
52. Cepeda V, Esteban M, Fraile-Ramos A. 2010. Human cytomegalovirus final envelopment on membranes containing both trans-Golgi network and endosomal markers. Cell Microbiol 12:386–404. https://doi.org/10.1111/j.1462-5822.2009.01405.x.
53. Krzyzaniak MA, Mach M, Britt WJ. 2009. HCMV-encoded glycoprotein M (UL100) interacts with Rab11 effector protein FIP4. Traffic 10:1439–1457. https://doi.org/10.1111/j.1600-0854.2009.00967.x.
54. Sanchez V, Greis KD, Sztul E, Britt WJ. 2000. Accumulation of virion tegument and envelope proteins in a stable cytoplasmic compartment during human cytomegalovirus replication: characterization of a potential site of virus assembly. J Virol 74:975–986. https://doi.org/10.1128/jvi.74.2.975-986.2000.
55. Das S, Pellett PE. 2011. Spatial relationships between markers for secretory and endosomal machinery in human cytomegalovirus-infected cells versus those in uninfected cells. J Virol 85:5864–5879. https://doi.org/10.1128/JVI.00155-11.
56. Kwon KM, Kim YE, Lee MK, Chung WC, Hyeon S, Han M, Lee D, Gong S, Ahn JH. 2021. Human cytomegalovirus UL48 deubiquitinase primarily targets innermost tegument proteins pp150 and itself to regulate their stability and protects virions from inclusion of ubiquitin conjugates. J Virol 95:e0099121. https://doi.org/10.1128/JVI.00991-21.
57. McCormick AL, Roback L, Wynn G, Mocarski ES. 2013. Multiplicity-dependent activation of a serine protease-dependent cytomegalovirus-associated programmed cell death pathway. Virology 435:250–257. https://doi.org/10.1016/j.virol.2012.08.042.
58. Andreoni M, Faircloth M, Vugler L, Britt WJ. 1989. A rapid microneutralization assay for the measurement of neutralizing antibody reactive with human cytomegalovirus. J Virol Methods 23:157–167. https://doi.org/10.1016/0166-0934(89)90129-8.